Journal of Applied Sciences

ISSN 1812-5654

science alert

ANSInet
an open access publisher
http://ansinet.com

Journal of Applied Sciences 11 (10): 1803-1808, 2011
ISSN 1812-5654 / DOI: 10.3923/jas.2011.1803.1808

Stress Analysis on Direct Joining of Sialon to AISI 430 Ferritic Stainless Steel

C.S. Hassan, P. Hussain and M. Awang
Department of Mechanical Engineering, University Teknology PETRONAS,
Bandar Seri Iskandar, 31750 Tronoh, Perak, Malaysia

Abstract: Finite Element Method (FEM) using ANSYS software was employed to evaluate the residual stress distribution in direct joining of sialon and AISI 430 ferritic stainless steel. The elastic-plastic model and four nodes quadratic element PLANE 42 with axisymmetric option were adopted in the analysis. Results showed that sialon experience compressive stresses in radial direction but tensile in axial direction. On the other hand, stresses in AISI 430 ferritic stainless steel are tensile in radial direction but compressive in axial direction. The highest tensile axial stress appeared at the radial free surface of sialon, very near to the joint interface. It is observed that shear stresses concentrated near and on the joint interface.

Key words: Ceramic, metal, joint, finite element method, residual stress

INTRODUCTION

Ceramic has been the material of choice for high temperature applications such as in internal combustion engine. In its application, ceramics are often in contact with metal. For example, in ceramic turbocharger rotors, each ceramic rotor requires attachment to a metal shaft, as illustrated by one of the rotors in Fig. 1 (Richerson, 2006). Ceramic/metal joint will take the advantage of metal toughness and the ability of ceramic to withstand high temperature. Furthermore, the brittleness of ceramic can also be overcome through this joining. However, successful ceramic/metal joints are difficult to obtain due to the rise of residual stresses in the joint. Residual stresses result from mismatches in the coefficient of thermal expansion and elastic modulus of the base materials. Upon cooling from the relatively high joining temperatures, characteristics of usual joining processes, the interface restricts the contraction of the material, concentrating local stresses (Martinelli, 1996). Such stresses can cause plastic deformation and cracking and thereby affect the mechanical integrity of the bonded materials (Lee and Kim, 1997).

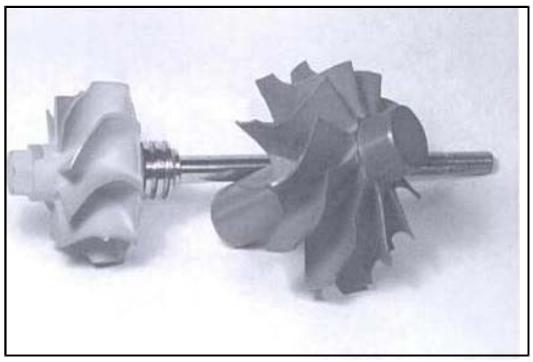

Fig. 1: Example of ceramic turbocharger rotors, one illustrating attachment to a metal shaft (Richerson, 2006)

Figure 2 shows the typical fracture mechanism that occurs in ceramic metal joint. When the joint is strong enough, mode I crack initiation occurs in the ceramic at this point. The stress becomes compressive soon after but maximum shear stress values are observed. As a consequence, mode I rapidly transforms to mode II crack propagation in the ceramic close and along the joint (Moret and Eustathopoulos, 1993; Lu and Evans, 1985). Mechanical attachments invariably result in residual stress concentration which may initiate cracks and cause failure (Hattali *et al*., 2009a). It must be pointed out that tensile stresses in the ceramic substrate, experimentally observed by X-ray diffraction, are harmful for the joint integrity since ceramic materials cannot withstand high tensile stress (Vila *et al*., 2005; Zhihong *et al*., 2009). Therefore, it is essential to evaluate the residual stress state in the joint.

An effective approach to predict and analyze the magnitude and distribution of the residual stresses along a joint based on the particular properties of the materials to be joined is the Finite Element s Method (FEM).

Corresponding Author: C.S. Hassan, Department of Mechanical Engineering, University Teknology PETRONAS, Bandar Seri Iskandar, 31750 Tronoh, Perak, Malaysia

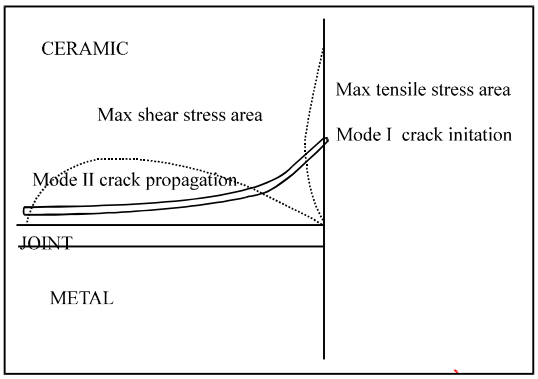

Fig. 2: Typical fracture mechanism of a ceramic/metal assembly. If the joint is strong enough, mode I crack initiation occurs on the lateral surface of the ceramic in the maximum tensile stress area and mode II crack propagation follows in the ceramic along the joint in the maximum shear stress area

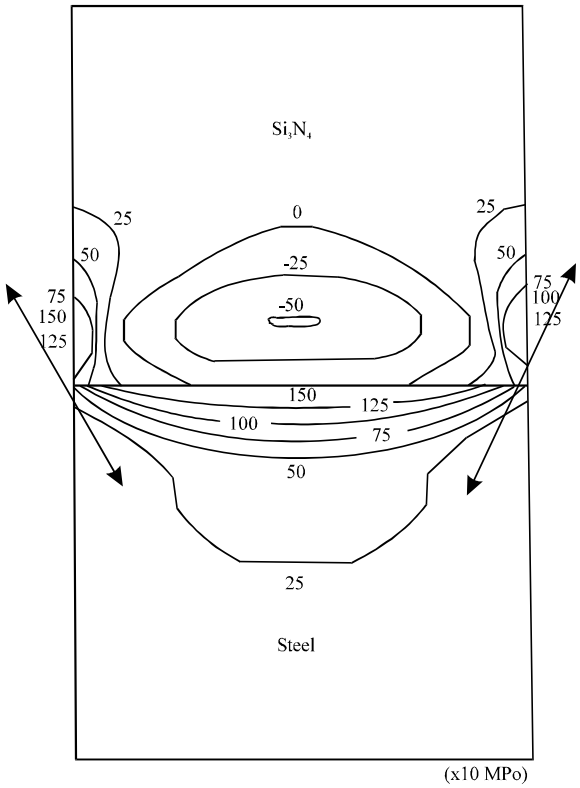

Fig. 3: Countermap of maximum principal stress calculated by FEM. The joint is assumed to be cooled from 1073K to room temperature fully elastically. The arrows indicate the position and direction of the maximum tensile stress (Suganuma *et al*., 1985)

Extensive studies had been carried out to study the residual stresses of ceramic-metal joints using FEM. According to, Travessa *et al.* (2002), once the bonding is obtained, the strength of the joint is primarily dependent on the residual stresses at the interface. These stresses, originated from the thermal expansion mismatch between the metallic and the ceramic substrates and constructed during the cooling down from the bonding temperature, were first quantified by analytical method (Virkar *et al*., 1987).

Later, FEM began to be applied not only to quantify residual stresses, but also to describe the stress field. Suganuma *et al.* (1985) had shown that maximum tensile stress concentrates on or near the interface and the free surface, as presented in Fig. 3. Xiaoqin *et al.* (2008) had calculated the residual stress distribution in Al_2O_3–TiC/W18Cr4V diffusion bonded joints using FEM. Vila *et al.* (2007) had used FEM calculations to simulate the joining process and residual strains of cube-shaped Ni/Si_3N_4 specimens. Williamson *et al.* (1995) had used FEM to study the effects of interlayer and creep in reducing residual stresses and strains in ceramic to metal joints. Several research works, such as by Drake *et al.* (1993) had used finite element numerical models and diffraction measurements to investigate residual stresses developed at bonded Al_2O_3-Ni interfaces. Raevska (1998) had also used FEM to study the dependence of residual stresses developed in ceramic metal joint on some design and technology parameters. Suganuma *et al.* (1984) by finite element analytical model, had showed that in joining dissimilar materials, there is formation of axial tensile stresses near the free surfaces of the materials with lower thermal expansion coefficient, adjacent to the interface, during cooling.

The key to successful numerical analyses relies on the selection of materials property, the proposed mechanisms for interface formation, and the development of elastic or elastic-plastic deformation models (Martinelli, 1996). The accuracy of FEM results further improved as elasto-plastic behavior of the metallic component started to be adopted in the model (Williamson *et al*., 1995).

MATERIALS AND METHODS

The aim of the present work is to numerically evaluate the magnitude and distribution of residual stresses in sialon/AISI 430 Ferritic Stainless Steel (FSS) joint by means of Finite Element Analysis (FEA). Sialon was chosen as they present excellent mechanical properties at high temperature. However, they cannot in general be use alone due to their brittleness. On the other hand, stainless steel is tough but operates at low temperature. Therefore,

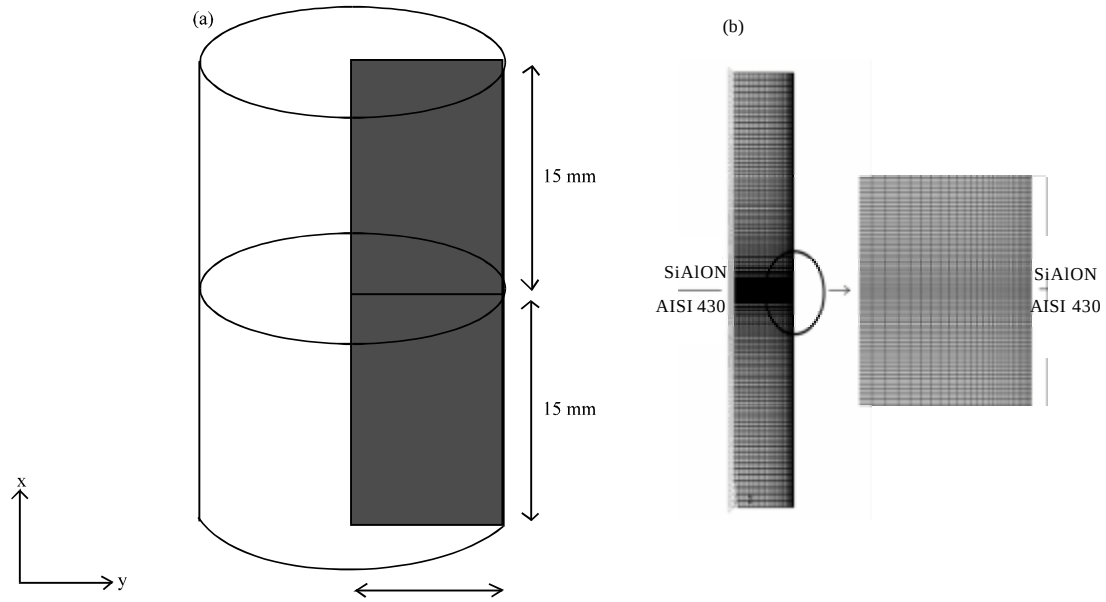

Fig. 4: Model description, (a) schematic representation of the model geometry resulted from the geometric simplification, showing the dimensions used in the analysis and (b) details on meshing and constrains employed

Table 1: Material properties of sialon and AISI 430 FSS employed in the analysis

Material	α (10^{-6} K^{-1})	E (GPa)	v	σ_y(MPa)
Sialon	3.1	300	0.22	
AISI 430	10.4	200	0.27	275

it is preferable to join them in order to utilize the strength of both materials.

FEA was applied to determine the magnitude and distribution of the residual stress in the sialon/AISI 430 FSS joint. The analysis was carried out using ANSYS 11 provided in the CAE/CFD lab of Universiti Teknologi PETRONAS. A cylindrical shaped AISI 430 FSS of 14 mm in diameter and 15 mm in thickness with 15 mm thickness of sialon on the top surface was considered. Sialon was treated as elastic while plasticity permitted within AISI 430 FSS. Elasto-plastic regime for the metal which governed by von Mises yield and isotropic hardening were adopted. Material response is assumed to be independent of time. Coefficient of thermal expansion (CTE), modulus of elasticity, poison's ratio as well as fracture and yield stress for sialon and AISI 430 FSS are given in Table 1.

Only thermal loading was employed to the model as sialon and stainless steel are assumed to be perfectly bonded at the interface at the fabrication temperature of 1200°C and stresses only developed during cooling down to room temperature. Since the model geometry is symmetrical in axial direction, the problem was analyzed as two-dimensional problem, as in Fig. 4. The four-node quadrilateral element PLANE42 with axisymmetric option has been used to model the joint. The model was imparted with mapped meshing with decreased element size as approaching the interface and free surface of the joint. The left boundary of the mesh corresponds to the symmetry axes were constrained in radial direction. All other boundaries remain free as to permit bending to occur during cooling. Details of meshing and constrains employed are in Fig. 4b.

RESULTS AND DISCUSSION

Figure 5 shows the distributions of radial, σ_x, axial, σ_y, and shear stresses, τ_{xy}, across the joint. With regards to specimen failure during cooling, the large tensile stresses within the ceramic near the radial free surface appear to be the most significant (Suganuma, 1990). This observation is consistent with the radial stresses distribution obtained by FEM, as in Fig. 5b. Do Nascimento et al. (2003) had stated that concentration of residual stress becomes severer as closing to the interface. The pattern of shear stresses distribution for sialon/ AISI 430 FSS joint agrees reasonably well with the statement. It can be seen in Fig. 5c that the shear stresses distribution concentrated on and near the interface of the joint. These stresses, in combination with the maximum axial tensile stress located at the free radial surface of sialon, clearly depicted the typical "concave/convex" fracture that sometimes observed in a joint with large thermal expansion mismatch (Do Nascimento *et al*., 2003).

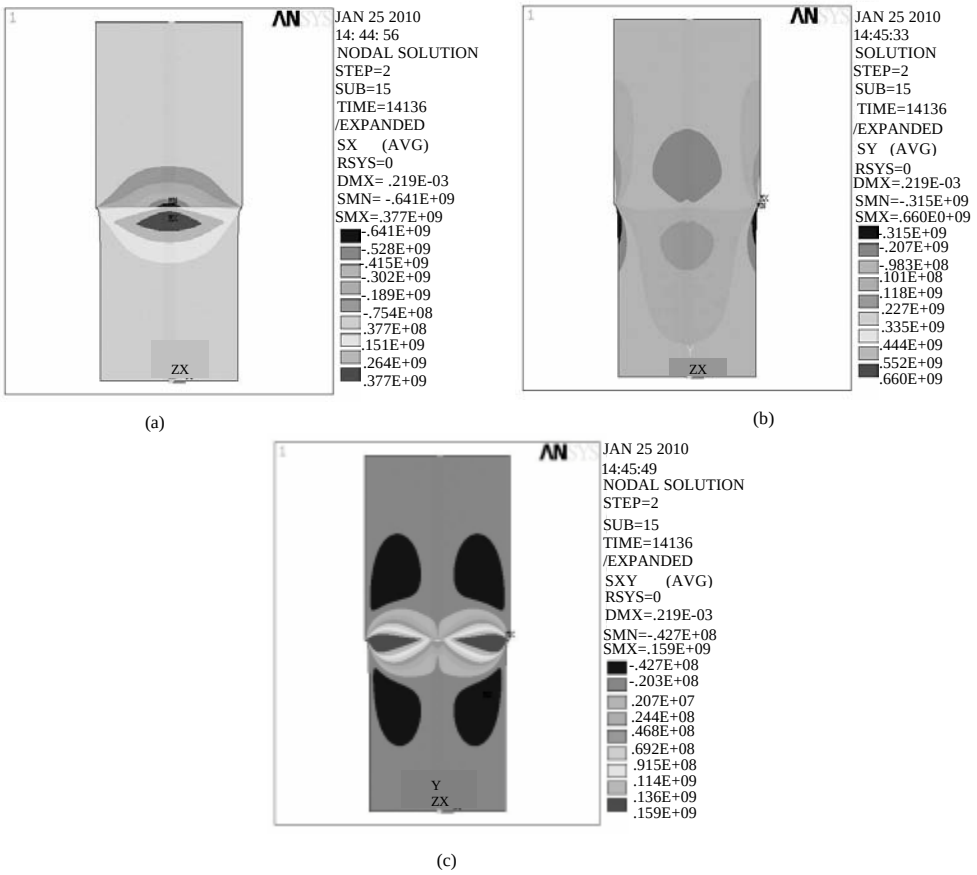

Fig. 5: Contour plots of the thermal residual stress distribution for the sialon/AISI 430 FSS joint: (a) radial stress (σ_x); (b) axial stress (σ) and (c) shear stress (τ_{xz})

In order to further analyze the magnitude and stress distribution across the joint, the stresses were plotted against the thickness of the seal. Radial stresses along the symmetry axes were plotted against thickness of the seal. Meanwhile, since axial and shear stresses rise to peak value at the radial free surface, stresses along the radial free surface were plotted against thickness of the seal. The plots of stresses magnitude against thickness are mentioned in Fig. 6. Thickness represented in Fig. 6 is measure from the bottom of the joint modeled. Thickness of AISI 430 FSS start from 0 up to the joint interface of 15 mm and thickness of sialon started right after the joint interface.

Figure 6a shows that, at the region near to the interface of the joint where thickness equal to 1.5 mm, high tensile stress developed in steel while ceramic experienced very low compressive stress. This is due to thermal expansion mismatch of AISI 430 FSS and sialon. AISI 430 FSS with higher CTE contracted more during cooling of the joint from the joining temperature. However, its contraction was restrained by its bonding to sialon, thus resulting in compressive stresses on the ceramic side. AISI 430 FSS reacted to that tendency, trying to extend the interface, yielding the concentration of tensile stresses, especially near the interface (Hattali et al., 2009a). The maximum radial tensile stress in the AISI 430 FSS is equal to 367.23 MPa while the minimum compressive stress in sialon is equal to 251.14 MPa. The stresses stabilize to nearly zero stresses when the distance is further away from the interface.

Figure 6b shows that axial stresses, represented as S_Y in ANSYS, are tensile in sialon while compressive in steel. The compressive stresses developed in AISI 430 FSS might be due to the effect of yielding of the steel (Cao *et al.*, 1988). The maximum axial stress is about 509.53 MPa located on the free surface of sialon, around 0.23 mm from the joint interface. This is belief to be the crack initiation point if any fracture occurs in the sialon/AISI 430 FSS joint. Cao *et al.* (1988) had stated that ceramic parts near the interface have high tensile residual stress and are prone to cracking. The cracks initiated at

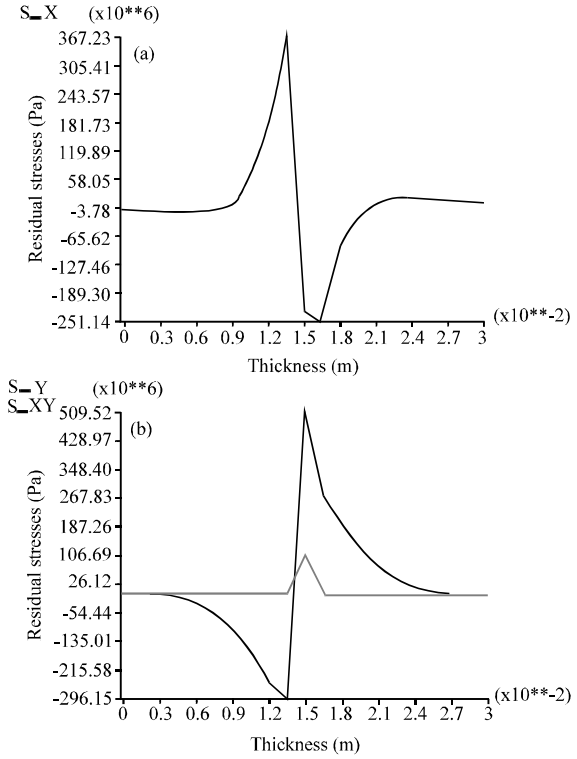

Fig. 6: Stress magnitude across sialon/ AISI 430 FSS joint, (a) radial stresses along the axis symmetry, and (b) axial and shear stresses along the radial free surface of the joint

the edge will downgrade the ceramic properties and may even lead to fracture. It can be seen that the amplitude of σ_y decreases as the distance from the interface decreases. On the sialon side, σ_y tensile stresses decreases and starts to stabilize to a nearly zero stresses at a distance of 1.1 mm away from the joint interface. Meanwhile, on the AISI 430 FSS side, σ_y is compressive in nature. The axial residual stresses decrease and achieved nearly zero magnitude of stress at a distance of 1.2 mm from the interface. The decreases of compressive σ_y in AISI 430 FSS might be as a result of the plastic deformation of the metal (Hattali *et al*., 2009b).

As can be seen in Fig. 6b, the tensile shear stresses, represented as S_XY in ANSYS, start developed in steel around 1.5 mm from the interface, and the stresses remain tensile in the ceramic up to around 1.5 mm from the interface. Maximum tensile shear stress of 106.69 Mpa developed at the sialon/ AISI 430 FSS joint interface. Also, it can be observed that on both sialon and AISI 430 FSS sides, like axial stresses, the amplitude of shear stresses also increase rapidly as approaching the joint interface and decreases to nearly zero stresses as moving further away from the interface.

Thermal expansion coefficient mismatch effect is a serious problem because, even if a strong interface could be achieved, joints with large residual stress are easily broken (Suganuma *et al*., 1987). The developments of residual stresses originated from the thermal expansion mismatch and induced during cooling down from the fabrication temperature strongly influence the joint integrity. Materials with low elastic modulus can accommodate strain and tend to deform under the influence of these stress. However, brittle material such as ceramic and glass will have a tendency to fracture. Sialon, like any other ceramic can bear with compressive stress but not tensile stress. They tend to fracture under the influence of high tensile stress. After evaluating all the stresses developed in the sialon/ AISI 430 FSS joint, it can be seen that the highest stress induced is the axial stress located in the free surface of the ceramic. In the case of sialon/ AISI 430 FSS joint with dimensions and fabrication temperature as described above, maximum axial tensile stress that developed in the sialon is equal to 509.53 Mpa. Even though the stress is considerably high, but the stress still did not exceed the ceramics' fracture stress of 825 MPa. This brings the possibility of successful direct joining of sialon to AISI 430 FSS.

CONCLUSION

The residual stresses generated in sialon/ AISI 430 FSS joint during cooling down from the fabrication temperature were predicted by the numerical model proposed. It was found that sialon experienced compressive stresses in axial direction but tensile in radial direction. On the other hand, AISI 430 FSS experienced tensile stress in radial direction but compressive in axial direction. Maximum tensile stress located on free radial surface of sialon, very near to the joint interface. It was also observed that shear stresses distribution concentrated on and near the interface of the joint. Since the maximum tensile stress developed in sialon did not exceed the fracture stress of the ceramic, it can be said that the joint is successful. Under specific conditions, joints can be obtained between sialon and AISI 430 FSS by means of bonding at the fabrication temperature of 1200°C. The magnitude and distribution of all stresses are stabilized to a very low stress as moving further away from the interface.

FEM had resulted in a very satisfactory description on magnitude and distribution of stresses in the ceramic/metal joint. Therefore numerical simulation can be used for assessing residual stress in ceramic/metal joint and as a guide in component fabrication. This method can be used as an alternative for trial and error experimental

work as it is more time saving and reducing material consumption. However, further experimental work is still recommended as to provide evidence for the FEM calculation.

ACKNOWLEDGEMENT

This research was made possible by a grant and facilities provided by Universiti Teknologi PETRONAS.

REFERENCES

Cao, H.C., M.D. Thouless and A.G. Evans, 1988. Residual stresses and cracking in brittle solids bonded with a thin ductile layer. Acta Metall., 36: 2037-2046.

Do Nascimento, R.M., A.E. Martinelli and A.J.A. Buschinelli, 2003. Review article: Recent advances in metal-ceramic brazing. Ceramica, 49: 178-179.

Drake, J.T., R.L. Williamson and B.H. Rabin, 1993. Finite element analysis of thermal residual stresses at graded ceramic/metal interfaces, part II: Optimization for residual stress reduction. J. Applied Phys., 74: 1321-1326.

Hattali, M.L., S. Terekhina, F. Ropital, N. Mesrati and D. Treheux, 2009a. Optimization of fabrication parameters of Alumina/Nickel alloy joints for high-temperature application. IOP Conf. Ser. Mater. Sci. Eng., 5: 012011-012011.

Hattali, M.L., S. Valette, F. Ropital, N. Mesrati and D. Treheux, 2009b. Effect of thermal residual stresses on the strength for both alumina/Ni/alumina and alumina/Ni/nickel alloy biomaterials. J. Mater. Sci., 44: 3198-3200.

Lee, S.B. and J.H. Kim, 1997. Finite-element analysis and X-ray measurement of the residual stresses of ceramic/metal joints. J. Mater. Process. Technol., 67: 167-172.

Lu, M.C. and A.G. Evans, 1985. Influence of cyclic tangential loads on indentation fracture. J. Am. Ceramic Soc., 68: 505-510.

Martinelli, A.E., 1996. Diffusion bonding of silicon carbide and silicon nitride to molybdenum. Ph.D. Thesis, McGill University, Canada.

Moret, F. and N. Eustathopoulos, 1993. Ceramic to metal direct brazing. J. Phys. IV, 3: C7-1043-C7-1052.

Raevska, S., 1998. Reduction of the stresses introduced during the diffusion bonding of dissimilar materials. J. Mater. Process. Technol., 77: 50-53.

Richerson, D.W., 2006. Modern Ceramic Engineering: Properties, Processing and Use in Design. 3rd Edn., Taylor and Francis Group, London.

Suganuma, K., 1990. Review: Recent advances in joining technology of ceramics to metals. ISU Int., 30: 1046-1058.

Suganuma, K., T. Okamoto and M. Koizumi, 1984. Effect of interlayers in ceramic-metal joints with thermal expansion mismatches. J. Am. Ceramic Soc., 67: C256-C257.

Suganuma, K., T. Okamoto, M. Koizumi and K. Kamachi, 1987. Influence of shape and size on residual stress in ceramic/metal joining. J. Mater. Sci., 22: 3561-3565.

Suganuma, K., T. Okamoto, M. Koizumi and M. Shimada, 1985. Effect of thickness on direct bonding of silicon nitride to steel. J. Am. Ceramic Soc., 68: 334-335.

Travessa, D., M. Ferrante and G. den Ouden, 2002. Diffusion bonding of aluminum oxide to stainless steel using stress relief interlayers. Mater. Sci. Eng. A, 337: 287-296.

Vila, M., C. Prieto, P. Miranzo, M.I. Osendi, J.M. Del Rio and J.L. Perez-Castellanos, 2005. Measurements and finite-element simulations of residual stress developed in Si3N4/Ni diffusion bonds. J. Am. Ceram. Soc., 88: 2515-2520.

Vila, M., C. Prieto, J. Zahr, J.L. Perez-Castellanos and G. Bruno *et al*., 2007. Residual stresses in ceramic-to-metal joints: Diffraction measurements and finite element method analysis. Philosophical Mag., 87: 5551-5563.

Virkar, A.V., J.L. Huang and R.A. Cutler, 1987. Strengthening of oxide ceramics by transformation-induced stress. J. Am. Ceramic Soc., 70: 164-170.

Williamson, R.L., B.H. Rabin and G.E. Byerly, 1995. FEM study on the effects of interlayers and creep in reducing residual stresses and strains in ceramic-metal joints. Composite Eng., 5: 851-863.

Xiaoqin, S., L. Yajiang, U.A. Putchkov, J. Wang and W. Huang, 2008. Finite-element analysis of residual stresses in Al2O3-TiC/W18Cr4V diffusion bonded joints. Comput. Mater. Sci., 45: 407-410.

Zhihong, Z., Z. Zhangjian and G. Changchun, 2009. Brazing of doped graphite to Cu using stress relief interlayers. J. Mater. Process. Technol., 209: 2662-2670.